

Semi-Asynchronous Federated Edge Learning for Over-the-air Computation

Zhoubin Kou¹, Yun Ji¹, Xiaoxiong Zhong^{1,2}, and Sheng Zhang^{1,*}

¹Graduate School in Shenzhen, Tsinghua University, Shenzhen, 518055, China

²Peng Cheng Laboratory, Shenzhen 518000, P.R. China

*Corresponding author: Sheng Zhang, email: zhangsh@sz.tsinghua.edu.cn

Abstract—Over-the-air Computation (AirComp) has been demonstrated as an effective transmission scheme to boost the efficiency of federated edge learning (FEEL). However, existing FEEL systems with AirComp scheme often employ traditional synchronous aggregation mechanisms for local model aggregation in each global round, which suffer from the stragglers issues. In this paper, we propose a semi-asynchronous aggregation FEEL mechanism with AirComp scheme (PAOTA) to improve the training efficiency of the FEEL system in the case of significant heterogeneity in data and devices. Taking the staleness and divergence of model updates from edge devices into consideration, we minimize the convergence upper bound of the FEEL global model by adjusting the uplink transmit power of edge devices at each aggregation period. The simulation results demonstrate that our proposed algorithm achieves convergence performance close to that of the ideal Local SGD. Furthermore, with the same target accuracy, the training time required for PAOTA is less than that of the ideal Local SGD and the synchronous FEEL algorithm via AirComp.

Index Terms—Federated edge learning, semi-asynchronous mechanism, over-the-air computation.

I. INTRODUCTION

With the advancement in computing capabilities and the accessibility of an unprecedented amount of data for portable devices, various machine learning based applications and services has been introduced to Internet of Thing (IoT) systems. However, the frequent data sharing of individual information in some services led to privacy concerns. Due to its appealing features of privacy protection, federated learning (FL) has been widely regarded as a promising machine learning technology [1]. Nevertheless, there are several problems to be addressed when deploying FL on wireless scenarios: 1) resource limitation: the total bandwidth and the transmission energy for all edge devices in wireless FL system are both finite; 2) heterogeneity: wireless FL suffers from the data heterogeneity and device heterogeneity, leading to global non-IID data distribution and different computing latency respectively.

In federated edge learning (FEEL) scenario, edge devices that collaborate to build a global model are often dispersed within a small physical range, and coordinated by a nearby parameter server (PS) [2]. A traditional approach for the uplink transmission of edge devices is to allocate channel resources through orthogonal access techniques, such as TDMA, CDMA and OFDMA. However, the limited wireless resources and large model data size in FEEL impose a

constraint on the number of edge devices that can participate in uploading.

Over-the-air computation (AirComp) has been proven to be an efficient paradigm to alleviate the communication costs and accelerate the FEEL training progress [3]. Leveraging the superposition property of wireless spectrum, AirComp can achieve uplink transmission of local models without the need for spectrum and time channel resource allocation.

To enhance the performance of wireless FEEL system, several studies related to the AirComp system for FEEL have been done [3]–[5]. A large amount of works follow the synchronous aggregation FEEL mechanism, where the parameter server (PS) does not update the global model until it receives local models from all the chosen edge devices in each global aggregation. However, in the common FEEL scenario of imbalanced computing ability among edge devices, following the synchronous aggregation mechanism for training FEEL can result in the risk of bottleneck nodes, while discarding the stragglers may need to lose important data. The former can prolong the training time of the model, and the latter can decrease the predictive accuracy of the final model.

In these circumstances, one potential solution is to apply the asynchronous mechanism into the FEEL. To fully take the advantage of high uplink throughput in AirComp, we propose a semi-asynchronous model aggregation mechanism with fixed interval time for global aggregation. The main contributions are summarized as follows:

- We propose a semi-asynchronous Periodic Aggregation Over-The-Air computation strategy named PAOTA under wireless multiple access channel (MAC) scenarios, which can utilize the waveform superposition property to realize AirComp during the wireless transmission.
- We analyze the convergence behavior of the semi-asynchronous FEEL via AirComp and derive the upper bound of the gap between the expected and optimal global loss values with respect to the transmission power. In PAOTA, the weighted parameters for model aggregation are proportional to the transmission power of the edge devices. To overcome the staleness in asynchronous aggregation and alleviate the data skewness caused by non-IID data, we transform the power control for uplink transmission into a trade-off optimization for the delay

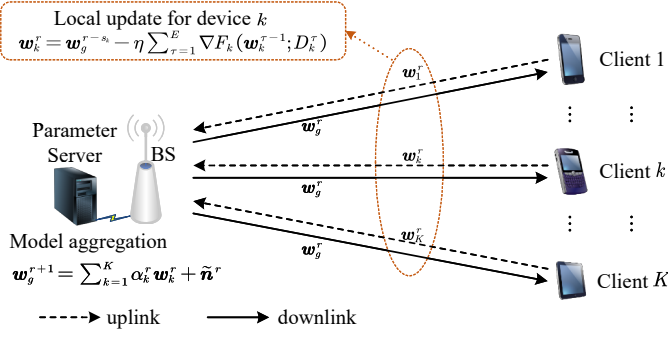


Fig. 1. FL system via wireless multiple-access channels.

factor of local model and the similarity factor of model gradient.

- The trade-off optimization problem is a nonlinear fractional programming of two convex quadratic functions. We solve it by using Dinkelbach's parametrization scheme. To optimize the nonconcave quadratic programming problem introduced by Dinkelbach's transform, we convert the problem into a 0-1 linear integer programming problem through piecewise linear approximation.
- According to the numerical results, PAOTA shows good training robustness under wireless FEEL system. Considering the heterogeneity of FEEL in the experiments, we verify the superiority of the algorithm PAOTA in terms of the predictive accuracy and the training time for converging to the target prediction accuracy.

II. SYSTEM MODEL

A. FL Problems

We consider a wireless FL system which consists of one parameter server and a set $\mathcal{K} = \{1, \dots, K\}$ of K edge devices, as shown in Fig. 1. Each client $k \in \mathcal{K}$ participating in the FL task is access to a local data set $\mathcal{D}_k = \{(\mathbf{x}_{k,1}, y_{k,1}), \dots, (\mathbf{x}_{k,D_k}, y_{k,D_k})\}$, with size $|\mathcal{D}_k| = D_k$. Then, the total set of data samples in the whole system can be denoted as $\mathcal{D} = \{\mathcal{D}_1, \dots, \mathcal{D}_K\}$, where size $D = \sum_{k=1}^K D_k$. $(\mathbf{x}_{k,i}, y_{k,i})$ is the i -th input-output pair stored in client k , where $\mathbf{x}_{k,i}$ denotes the feature vector and $y_{k,i}$ denotes the corresponding label value. The goal of FL task is to minimize the global loss function by training global model parameter \mathbf{w} , where the local data samples at edge devices are unavailable to the PS on account of the privacy concern. The optimization problem of FL can be formulated as follow:

$$\min_{\mathbf{w}} F(\mathbf{w}) = \sum_{k=1}^K \frac{D_k}{D} F_k(\mathbf{w}), \quad (1)$$

where F_k is the local loss function defined as

$$F_k(\mathbf{w}) = \frac{1}{D_k} \sum_{i \in \mathcal{D}_k} l(\mathbf{w}; (\mathbf{x}_{k,i}, y_{k,i})), \quad (2)$$

where $l(\mathbf{w}; (\mathbf{x}_{k,i}, y_{k,i}))$ is the empirical loss function.

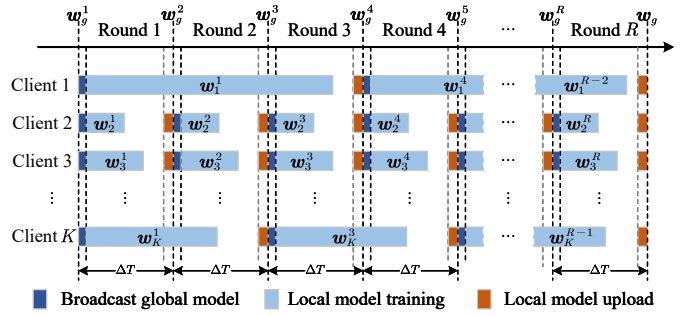


Fig. 2. The work-flow of federated learning with periodic aggregation.

B. Semi-asynchronous FL with Periodic Aggregation

Inspired by [8], we propose a time-triggered semi-asynchronous aggregation. The work-flow of our proposed PAOTA is shown in Fig. 2. The global aggregation proceeds periodically, and the interval time of each cycle ΔT remains constant. We assume R rounds of FL training are performed, and use vector $\mathbf{b}^r = [b_1^r, \dots, b_K^r] \in \{0, 1\}$ to indicate the state information of K edge devices. After the PS broadcasts the model to client k , the element of state vector b_k^r is assigned as zero at first. When client k finishes its local training at the r -th round, it sends a signal to the server showing that client k is ready to upload its local model. Then the PS will set the value of b_k^r to 1, which means client k will attend the global aggregation at r -th round and be ready to receive the updated global model at the beginning of the $(r+1)$ -th round.

C. Asynchronous Aggregation via AirComp

In this paper, we consider the scenario where the downlink communication is error-free. The uplink channels remain unchanged when edge devices transmit local models to the PS at one round, and the wireless MAC channels are adopted. Following the Rayleigh distribution, the uplink channels are independent across different transmission rounds.

We assume the PS will carry out R rounds of iterations in total for a FL task. At the r -th ($r \in \{1, \dots, R\}$) round of global training iteration:

(a) **Global model broadcasting.** At the beginning of each global round, the PS broadcasts the global model \mathbf{w}_g^k to edge devices according to the edge devices state vector $\mathbf{b}^r = [b_1^r, \dots, b_K^r] \in \{0, 1\}$. When client k does not complete the local training of the previous global round, set $b_k^r = 0$; and when client k is ready to participate in the FL task at the r -th round, $b_k^r = 1$. In particular, the PS broadcasts global model \mathbf{w}_g^1 to all edge devices at the first global round, which means $b_k^1 = 1, \forall k$. Since the downlink communication is assumed to be a perfect transmission, each client can get the global model without transmission errors.

(b) **Local model training.** If $b_k^r = 1$, client k receives the global model \mathbf{w}_g^r and use stochastic gradient decent (SGD) to update local model based on their own datasets \mathcal{D}_k . We assume each client runs M rounds iterations for local model

training, at the m -th local update, $m \in \{1, \dots, M\}$, the local model $\mathbf{w}_{k,m}^r$ is formed as

$$\mathbf{w}_{k,m}^r = \mathbf{w}_g^r - \eta \sum_{\tau=1}^m \nabla F_k(\mathbf{w}_{k,\tau-1}^r; D_k^r), \quad (3)$$

where η is the learning rate, D_k^m is the data used in the m -th round of local training. If $b_k^r = 0$, client k will keep training the local model which haven't been finished at the previous round. We define s_k^r as the number of rounds that client k falls behind the global training round, then the update of straggler k can be expressed as

$$\mathbf{w}_{k,m}^{r,s_k^r} = \mathbf{w}_g^{r-s_k^r} - \eta \sum_{m=1}^M \nabla F_k(\mathbf{w}_{k,m-1}^{r,s_k^r}; D_k^m), \quad (4)$$

As we can see, (3) is a special case of (4) when s_k^r equals to 0. After M SGD training iterations, client k finishes its local training at r -th global round and the updated local model is denoted as $\mathbf{w}_{k,M}^{r,s_k^r}$.

(c) **Local model upload.** In this paper, we assume that the wireless AirComp can achieve strict clock synchronization, called alignment over-the-air computation, so that edge devices' signals overlap exactly with each other at the PS.

The edge devices who complete their local training during r -th global round will transmit their local model through AirComp at the same period, as shown in Fig. 2. Assuming the channel state information (CSI) is known by all the edge devices and the PS perfectly, we consider a pre-processing parameter ϕ_k^r for the transmitter of the edge devices which is denoted by

$$\phi_k^r = \frac{b_k^r p_k^r (h_k^r)^H}{|h_k^r|^2}, \quad (5)$$

where $h_k^r \in \mathbb{C}$ is the complex channel coefficient of the uplink transmission between client k and the PS, p_k^r is the transmit power of client k , and $(\cdot)^H$ represents conjugate transpose.

The transmit signal of client k can be expressed as $\mathbf{x}_k^r = \phi_k^r \mathbf{w}_{k,M}^{r,s_k^r}$. As the PS knows the perfect CSI, the received signal of PS can be formulated as

$$\mathbf{y}_g^r = \sum_{k=1}^K h_k^r \mathbf{x}_k^r + \mathbf{n}^r = \sum_{k=1}^K b_k^r p_k^r \mathbf{w}_{k,M}^{r,s_k^r} + \mathbf{n}^r, \quad (6)$$

where $\mathbf{n}^r \in \mathbb{C}^d$ represents the independent identical distribution (i.i.d) additive Gaussian white noise (AWGN) following the distribution $\mathcal{CN}(0, \sigma_n^2 \mathbf{I})$. And $\sigma_n^2 = B N_0$, where B is the bandwidth of uplink channel, and N_0 represents the channel noise power spectral density. For limited power of each client, we have:

$$\|\phi_k^r \mathbf{w}_{k,M}^{r,s_k^r}\|_2^2 \leq P_{k,\max}^r, \quad (7)$$

where $P_{k,\max}^r$ is the maximum power of client k at the r -th round.

(d) **Global model update.** After the upload time slot of each global round, the PS receives the aggregation signal through AirComp, and performs a normalization operation to obtain the updated global model \mathbf{w}_g^{r+1}

$$\begin{aligned} \mathbf{w}_g^{r+1} &= \frac{\mathbf{y}_g^r}{\zeta^r} = \sum_{k=1}^K \frac{b_k^r p_k^r}{\zeta^r} \mathbf{w}_{k,M}^{r,s_k^r} + \frac{\mathbf{n}^r}{\zeta^r} \\ &= \sum_{k=1}^K \alpha_k^r \mathbf{w}_{k,M}^{r,s_k^r} + \tilde{\mathbf{n}}^r, \end{aligned} \quad (8)$$

where ζ^r is the normalization factor at r -th round and can be calculated by $\zeta^r = \sum_{k=1}^K b_k^r p_k^r$. Then the actual weight parameter of client k can be formulated by $\alpha_k^r = \frac{b_k^r p_k^r}{\sum_{i=1}^K b_i^r p_i^r}$ for simplicity, where α_k^r satisfies $\sum_{k=1}^K \alpha_k^r = 1$. $\tilde{\mathbf{n}}^r$ is the equivalent noise after the normalization operation.

To facilitate the derivation of convergence, we further express global model aggregation as follow:

$$\mathbf{w}_g^{r+1} = \tilde{\mathbf{w}}^r + \sum_{k=1}^K \alpha_k^r \Delta \mathbf{w}_k^r + \tilde{\mathbf{n}}^r, \quad (9)$$

where $\tilde{\mathbf{w}}^r = \sum_{k=1}^K \alpha_k^r \mathbf{w}_g^{r-s_k^r}$ represents the weighted sum of the global model parameters based on the users participating in uploading the local model during r -th round of aggregation, and $\Delta \mathbf{w}_k^r = -\eta \sum_{\tau=1}^E \nabla F_k(\mathbf{w}_{k,\tau-1}^{r,s_k^r}; D_k^r)$ is the local update of client k at the r -th round.

III. CONVERGENCE ANALYSIS AND OPTIMIZATION ALGORITHM

In this section, we analyze how the wireless MAC environment and the periodic aggregation strategy affect the convergence behavior of PAOTA presented in Section II. Firstly, we derive the upper bound of the expected optimal gap between the expected and optimal global loss values. Then, combining with the characteristics of the asynchronous mechanism and data heterogeneity, we minimize the derived upper bound by optimizing the parameter β related to the staleness factor and the gradient similarity factor. The whole process of PAOTA is shown in **Algorithm 1**.

A. Convergence Analysis

We present the following assumptions and lemmas that are necessary when we derive the convergence behavior of PAOTA algorithm at first.

Assumption 1: The global loss function F is L -smooth, i.e., $\forall \mathbf{x}, \mathbf{y}$:

$$F(\mathbf{x}) - F(\mathbf{y}) \leq (\mathbf{x} - \mathbf{y})^T \nabla F(\mathbf{y}) + \frac{L}{2} \|\mathbf{x} - \mathbf{y}\|_2^2, \quad (10)$$

$$\|\nabla F(\mathbf{x}) - \nabla F(\mathbf{y})\| \leq L \|\mathbf{x} - \mathbf{y}\|, \quad (11)$$

Assumption 2 [9]: The variance of the local model gradients at each local device is bounded by ζ :

$$\mathbb{E} \left[\|\nabla F_k(\mathbf{w}_k^r) - \nabla F(\mathbf{w}_g^r)\|_2^2 \right] \leq \zeta, \quad (12)$$

where ζ is the parameter related to the data heterogeneity.

These two assumptions above are widely used in the convergence analysis for traditional synchronous FL. **Assumption 1** makes sure the gradient of F does not change quickly during global training. And the **Assumption 2** captures the degree of data heterogeneity by parameter ζ .

Assumption 3 [8]: The global model gradient change within n training rounds is bounded as

$$(\mathbf{w}_g^{r-n} - \mathbf{w}_g^r)^T \nabla F(\mathbf{w}_g^r) \leq \delta \|\nabla F(\mathbf{w}_g^r)\|_2^2, \quad (13)$$

$$\|\mathbf{w}_g^{r-n} - \mathbf{w}_g^r\| \leq \epsilon, \quad (14)$$

where δ and ϵ are constant value. And the local model gradient change within m local rounds is bounded as

$$\|\nabla F(\mathbf{w}_k^{r-m})\| \leq \vartheta \|\nabla F(\mathbf{w}_k^r)\|, \quad (15)$$

where ϑ is a constant value.

Assumption 4 : The SGD algorithm performed by the edge device is unbiased, i.e.,

$$\mathbb{E}[\nabla F_k(\mathbf{w}_k; \mathcal{D}_k)] = \nabla F_k(\mathbf{w}_k), \quad (16)$$

and the variance of stochastic gradients at each edge device is bounded as

$$\mathbb{E}[\|\nabla F_k(\mathbf{w}_k; \mathcal{D}_k) - \nabla F_k(\mathbf{w}_k)\|_2^2] \leq \sigma^2, \quad (17)$$

where σ is a constant value.

Lemma 1: The sum of the expected square norm of the difference between the local updated model at each SGD iteration and the previous global model is bounded by

$$\begin{aligned} & \sum_{\tau=1}^M \mathbb{E}[\|\mathbf{w}_g^{r-s_k^\tau} - \mathbf{w}_k^{r-s_k^\tau, \tau-1}\|_2^2] \\ & \leq \frac{\eta_t^2 M^3 \sigma^2 + 4\eta_t^2 M^3 L^2 \zeta + 4\eta_t^2 M^3 \beta^2 \mathbb{E}[\|\nabla F(\mathbf{w}_g^r)\|_2^2]}{1 - 2\eta^2 M^2 L^2}, \end{aligned} \quad (18)$$

Proof: See the section Appendix A. ■

Lemma 2: For a L -smooth function F with optimum solution \mathbf{w}^* , the following inequality holds

$$\|\nabla F(\mathbf{w})\|_2^2 \leq 2L(F(\mathbf{w}) - F(\mathbf{w}^*)), \quad (19)$$

Proof: As F is a L -smooth function, for \mathbf{w} and the optimum solution \mathbf{w}^* , we have

$$\begin{aligned} & \frac{1}{2L} \|\nabla F(\mathbf{w}) - \nabla F(\mathbf{w}^*)\|_2^2 \\ & \leq F(\mathbf{w}) - F(\mathbf{w}^*) - (\mathbf{w} - \mathbf{w}^*)^T \nabla F(\mathbf{w}^*), \end{aligned} \quad (20)$$

where $\nabla F(\mathbf{w}^*) = 0$. Rearrange the (20) and we can get the (19). ■

Now, we present the main convergence analysis result in the following theorem. Now, we present the main convergence analysis result in the following theorem.

Theorem 1: The expected optimal gap between the expected and optimal global loss values is bounded as

$$\begin{aligned} & \mathbb{E}[F(\mathbf{w}^{R+1})] - F(\mathbf{w}^*) \\ & \leq \prod_{r=1}^R A^r \mathbb{E}[F(\mathbf{w}_g^1) - F(\mathbf{w}^*)] + G^R \\ & \quad + \sum_{r=1}^R \left(\prod_{i=r+1}^R A^i \right) G^r, \end{aligned} \quad (21)$$

where

$$\begin{aligned} A^r & = 1 + 2L\delta - L\eta M + 8L^2\eta^2 M\vartheta^2 \\ & \quad + (\eta L^2 + 4M\eta^2 L^3) \frac{8L\eta^2 M^3 \vartheta^2}{1 - 2\eta^2 M^2 L^2}, \end{aligned} \quad (22)$$

and

$$\begin{aligned} G^r & = \underbrace{(2\eta M + 8L\eta M^2 + \frac{4\eta^2 M^3 L^2 (\eta L^2 + 4M\eta^2 L^3)}{1 - 2\eta^2 M^2 L^2})}_{(a)} \zeta + \\ & \quad \underbrace{2\eta M L^2 \epsilon^2}_{(b)} + \underbrace{(2\eta^2 L M^2 + \frac{(\eta L^2 + 4M\eta^2 L^3) \eta^2 M^3}{1 - 2\eta^2 M^2 L^2})}_{(c)} \sigma^2 \\ & \quad + \underbrace{L\epsilon^2 K \sum_{k=1}^K (\alpha_k^r)^2}_{(d)} + \underbrace{\frac{2Ld\sigma_n^2}{(\sum_{k=1}^K b_k^r p_k^r)^2}}_{(e)}, \end{aligned} \quad (23)$$

Proof: Due to space limitations, please see Appendix A in the extended version [10]. ■

According to the **Theorem 1**, we can learn that the upper bound of $\mathbb{E}[F(\mathbf{w}^{R+1})] - F(\mathbf{w}^*)$ depends only on the second term G^r given a sufficient number of iteration rounds, as long as the setting of learning rate η satisfies $A(t) < 1$.

It is natural to think of minimizing the value of G^r by adjusting the controllable parameters in the wireless FL system. As shown in (23), G^r consists of 5 terms (a)-(e): the terms (a)-(c) are only dependent on the hyper-parameters that relate to the wireless FL system settings, which can not change during the training iterations. Term (d) and term (e) contain the upload transmit power value p_k , which control the aggregation weight of the local models uploaded by different edge devices.

To sum up, there are two kinds of factors affecting the global model convergence in our proposed system. On the one hand, the asynchronous aggregation process introduces stale models to global update, thus impairing the convergence speed of FEEL. On the other hand, the noise present in the wireless transmission environment negatively impacts the convergence performance of federated learning.

B. Power Control Optimization

Based on the **Theorem 1**, we can minimize the upper bound of $\mathbb{E}[F(\mathbf{w}^{R+1})] - F(\mathbf{w}^*)$ by optimizing the terms (d) and (e) through the uplink transmit power p_k , $k = 1, \dots, K$. By dropping the notation r for simplicity, the optimal problem can be formulated as:

$$\mathbf{P1} : \min_{p_1, \dots, p_K} L\epsilon^2 K \sum_{k=1}^K \alpha_k^2 + \frac{2Ld\sigma_n^2}{(\sum_{k \in \mathcal{K}} b_k p_k)^2} \quad (24a)$$

$$\text{s.t. } p_k \leq P_{\max}^k, k = 1, \dots, K, \quad (24b)$$

where $\mathbf{p} = [p_1, \dots, p_K] \in R^{1 \times K}$ is the transmission power of K clients.

Different with synchronous FL, PAOTA has to suffer the impact of the stale information. Meanwhile, the problem of data bias introduced by the non-IID data distribution also should be considered. As the model aggregation weights is

Algorithm 1 PAOTA

Require: Global training rounds R ; Time duration of each round ΔT ; Local training rounds E ; Uplink power budget of each client p_k^{\max} ; Initial global model w_g^0 ; State Tag of each client $b_k^0 = 1, \forall k$;

- 1: **for** $r = 0, 1, \dots, R - 1$ **do**
- 2: PS broadcasts w_g^r to clients k satisfying $b_k = 1, \forall k$;
- 3: Set $b_k \leftarrow 0$;
- 4: **for** $k = 1, \dots, K$ in parallel **do**
- 5: **for** $\tau = 1, \dots, M$ **do**
- 6: $w_k^{r, \tau+1} \leftarrow w_k^{r, \tau} - \eta \nabla F_k(w_k^{r, \tau}; D_k^{\tau+1})$;
- 7: **if** $\tau = M$ **then**
- 8: $b_k \leftarrow 1$;
- 9: Obtain current round value r' , uplink channel gains $h_k^{r'}$ and parameter $\beta^{r'}$;
- 10: Set the $\phi_k^{r'}$ based on (5) and (25);
- 11: Transmit the signal $x_k^{r', r'-r} = \phi_k^{r'} w_{k,E}^{r'}$ at the aggregation time slot of round r' ;
- 12: **end if**
- 13: **end for**
- 14: **end for**
- 15: PS receives MAC signal (6) at the aggregation time slot, performs the normalization operation based on (8) and obtains the updated global model w_g^{r+1} ;
- 16: **end for**

determined by the uplink transmission power directly according to (8), we represent the power parameter as follow:

$$\begin{aligned}
 p_k &= p_k^{\max} \cdot \beta_k \cdot \frac{\Omega}{s_k + \Omega} \\
 &+ p_k^{\max} \cdot (1 - \beta_k) \cdot \frac{\Theta(\Delta w_k^t, w_g^t - w_g^{t-1}) + 1}{2} \quad (25) \\
 &= p_k^{\max} (\beta_k \cdot \rho_k + (1 - \beta_k) \cdot \theta_k),
 \end{aligned}$$

where s_k is the staleness factor of local model w_k at each round, θ_k is the interference factor of local model, Ω is a constant to limit the maximum degree of latency, and $\Theta(\mathbf{a}, \mathbf{b}) \in [-1, 1]$ represents the cosine of the angle between two vector \mathbf{a} and \mathbf{b} . $\beta_k \in [0, 1]$ is a hyper-parameter that can make a trade-off between the staleness factor ρ_k and the interference factor θ_k [7], and makes p_k still subject to the individual transmit power condition (7) where $0 \leq p_k \leq p_k^{\max}$.

By substituting the expression for p_k into the original optimization problem **P1** and representing it in matrix form, we obtain the final optimization problem:

$$\mathbf{P2} : \min_{\beta} \frac{(\theta + D\beta)^T P_{\max}^T \Theta P_{\max} (\theta + D\beta) + 2Ld\sigma_u^2}{(\theta + D\beta)^T P_{\max}^T I I^T P_{\max} (\theta + D\beta)} \quad (26a)$$

$$\begin{aligned}
 &= \frac{\beta^T G \beta + \mathbf{g}^T \beta + g_0}{\beta^T Q \beta + \mathbf{q}^T \beta + q_0} = \frac{h_1(\beta)}{h_2(\beta)} \quad (26a) \\
 \text{s.t. } &\beta_k \in [0, 1], k = 1, \dots, K, \quad (26b)
 \end{aligned}$$

where $\rho^T = [\rho_1, \dots, \rho_K]$, $\theta^T = [\theta_1, \dots, \theta_K]$, $\beta^T = [\beta_1, \dots, \beta_K]$, $P_{\max} = \text{diag}\{p_1^{\max}, \dots, p_K^{\max}\}$ and $D = \text{diag}\{\rho_1 - \theta_1, \dots, \rho_K - \theta_K\}$. $Q =$

$D^T P_{\max}^T \Theta P_{\max} D$ is a $K \times K$ symmetric positive definite matrix, $G = D^T P_{\max}^T \Theta^T P_{\max} D$ is a $K \times K$ symmetric positive semi-definite matrix, $\mathbf{q} = 2\theta^T P_{\max}^T \Theta P_{\max} D$, $\mathbf{g} = 2\theta^T P_{\max}^T \Theta^T P_{\max} D$ are K -vectors. $q_0 = \theta^T P_{\max}^T \Theta P_{\max} \theta$, $g_0 = \theta^T P_{\max}^T \Theta^T P_{\max} \theta + 2Ld\sigma_u^2$ are constants.

Problem (26) is a nonlinear fractional programming problem, where both the dividend and divisor are convex quadratic functions subject to linear constraints. To solve this problem, we adopt an improved version of the Dinkelbach's algorithm [6], as shown in **Algorithm 2**. The Dinkelbach's transform of problem **P2** can be formulated as:

$$\mathbf{P3} : \max_{\beta} F(\beta; \lambda) = h_2(\beta) - \lambda h_1(\beta) \quad (27a)$$

$$\text{s.t. } \beta_k \in [0, 1], k = 1, \dots, K. \quad (27b)$$

where $\lambda > 0$ is treated as a parameter. And **P3** is a maximization of a non-concave quadratic function. Now, we apply the standard piecewise linear approximation of quadratic functions and reformulate **P3** as a 0-1 linear integer programming problem. Since G is symmetric and positive definite, there exists a nonsingular matrix M_1 such that $G = M_1^T M_1$. Let $\beta = M_1 \beta$. Then

$$F(\beta; \lambda) = \mathbf{y}^T S \mathbf{y} - \lambda \mathbf{y}^T \mathbf{y} + (\mathbf{q}^T - \lambda \mathbf{g}^T) \beta + (q_0 - \lambda g_0), \quad (28)$$

and since Q is symmetric and positive semi-definite, there exists an orthogonal matrix M_2 such that $M_2^T S M_2 = N$, $M_2^T M = I$, where $N = \text{diag}(n_i)$. Therefore, we have

$$\begin{aligned}
 F(\beta; \lambda) &= \beta^T M_1^T M_2 (N - \lambda I) M_2^T M_1 \beta \\
 &+ (\mathbf{q}^T - \lambda \mathbf{g}^T) \beta + (q_0 - \lambda g_0), \quad (29)
 \end{aligned}$$

Problem **P3** can be represented as follow:

$$\mathbf{P4} : \max_{\beta} f(\beta; \lambda) = \mathbf{z}^T (N - \lambda I) \mathbf{z} + (\mathbf{q}^T - \lambda \mathbf{g}^T) M^{-1} \mathbf{z} + (q_0 - \lambda g_0) \quad (30a)$$

$$\text{s.t. } \beta_k \in [0, 1], k = 1, \dots, K, \quad (30b)$$

$$\mathbf{z} = M \beta, \quad (30c)$$

where $M = M_2^T M_1$. Now, let

$$\mathbf{Z} = \{\mathbf{z} \in \mathbb{R}^n | M^{-1} \mathbf{z} = \beta\} \quad (31)$$

and let

$$z_{i\varrho+1} = \max\{z_i | \mathbf{z} \in \mathbf{Z}\}, i = 1, 2, \dots, n, \quad (32)$$

$$z_1 = \min\{z_i | \mathbf{z} \in \mathbf{Z}\}, i = 1, 2, \dots, n, \quad (33)$$

We split the interval $[z_1, z_{i\varrho+1}]$ into m sub-intervals of equal length. The piecewise linear approximation of the objective function can be represented by introducing a number of auxiliary variables γ_{ij} , $i = 1, 2, \dots, n$ and $j = 1, 2, \dots, \varrho + 1$, as follows:

$$\begin{aligned}
 \mathbf{z}^T (N - \lambda I) \mathbf{z} &= - \sum_{i=1}^{n-h} c_i(\lambda) \sum_{j=1}^{\varrho+1} z_{ij}^2 \gamma_{ij} \\
 &+ \sum_{i=n-h+1}^n c_i(\lambda) \sum_{j=1}^{\varrho+1} z_{ij}^2 \gamma_{ij} \quad (34)
 \end{aligned}$$

Algorithm 2 Dinkelbach's Method

Require: tolerance ε ; λ_0 satisfying $F(\beta; \lambda_0) \geq 0$; iteration number $n = 0$;

- 1: **repeat**
- 2: set $\lambda = \lambda_n$
- 3: Solve 0-1 MIP Problem (39) derived from (27)'s piece-wise linear approximation to obtain β^* ;
- 4: $\lambda_{n+1} \leftarrow \frac{h_2(\beta^*)}{h_1(\beta^*)}$;
- 5: $n \leftarrow n + 1$;
- 6: **until** $F(\beta; \lambda_n) \leq \varepsilon$

$$z_i = \sum_{j=1}^{\varrho+1} z_{ij} \gamma_{ij}, i = 1, 2, \dots, n, \quad (35)$$

$$\sum_{j=1}^{\varrho+1} \gamma_{ij} = 1, i = 1, 2, \dots, n, \quad (36)$$

$$\gamma_{ij} \geq 0, i = 1, 2, \dots, n \text{ and } j = 1, 2, \dots, \varrho + 1 \quad (37)$$

Let us note that we need to introduce the 0-1 variables c_{ij} , $i = n - j + 1, \dots, n$ for $j = 1, 2, \dots, \varrho$,

$$\begin{aligned} \gamma_{i1} &\leq c_{i1}, \\ \gamma_{i2} &\leq c_{i1} + c_{i2}, \\ &\vdots \\ \gamma_{i\varrho} &\leq c_{ih-1} + c_{ih}, \\ \sum_{j=1}^m y_{ij} &= 1, \end{aligned} \quad (38)$$

Therefore, the 0-1 linear integer programming problem can be reformulated as follow:

$$\begin{aligned} \max_{\mathbf{z}} \quad & - \sum_{i=1}^{n-h} c_i(\lambda) \sum_{j=1}^{\varrho+1} z_{ij}^2 \gamma_{ij} + \sum_{i=n-h+1}^n c_i(\lambda) \sum_{j=1}^{\varrho+1} z_{ij}^2 \gamma_{ij} \\ & + (\mathbf{q}^T - \lambda \mathbf{g}^T) \mathbf{M}^{-1} \mathbf{z} + (q_0 - \lambda g_0) \end{aligned} \quad (39a)$$

$$\text{s.t. } \mathbf{z} \in \mathcal{Z}, \quad (39b)$$

$$(34), (35), (36), (37), (38).$$

This is a mixed integer programming problem with $h \times \varrho$ 0-1 variables which can be solved by IBM CPLEX Optimizer efficiently. And then we can get the optimal β by using (30c) and the solution of the problem **P1** by adopting (25).

IV. SIMULATION RESULTS

A. Experiment Settings

We consider a cellular network consisting of a basic station (BS) and 100 clients participating in FEEL training, where the downlink transmission is error-free. The maximal transmit power of local devices is $p_{\max}^k = 15\text{w}$. We set the uplink transmission bandwidth as 20MHz, and the channel noise power spectral density as $N_0 = -174\text{dBm/Hz}$. And we set $M = 5$, $L = 10$, and $\Omega = 3$. We train a multi-layer perceptron (MLP) network which has two hidden layers with 10 nodes on the MNIST dataset. Considering the non-IID distribution

among each clients, we set the number of training samples in different clients varies from $\{300, 600, 900, 1200, 1500\}$ and each device contains five categories of digit images at most.

In order to realize the heterogeneity of edge devices in the computing ability, we set the computation latency of each client during different local training round to follow the uniform distribution $\mathcal{U}(5, 15)$ s, and the period of model aggregation at each epoch for PAOTA as $\Delta T = 8\text{s}$.

B. Performance Comparison

We compare the proformance of PAOTA algorithm with the following federated learning algorithms:

(1) Local SGD [1]: An ideal synchronous federated learning algorithm, where each user transmits its local model without considering transmission loss.

(2) COTAF [3]: One of the classic AirComp based FEEL algorithms where each user transmits its model updates through the MAC and performs time-varying pre-coding.

For fairness consideration, we set an equal number of participating clients for each round of training in the three algorithms. To verify the effectiveness of the proposed algorithm, we first numerically evaluate the gap between expected objective and optimal loss function value, i.e., $\mathbb{E}[F(\mathbf{w}^r)] - F(\mathbf{w}^*)$.

As shown in Fig. 3, we observe that PAOTA can achieve convergence speed close to Local SGD when $N_0 = -174\text{dBm/Hz}$. This verifies that the PAOTA algorithm can effectively compensate for the negative impact of additive noise and asynchronous aggregation mechanism on model convergence speed. Moreover, as the number of iterations increases, PAOTA can achieve a smaller gap than Local SGD, indicating that PAOTA improves the utilization of heterogeneous data in clients through the proposed semi-asynchronous aggregation strategy.

Furthermore, in Fig. 3, both COTAF and PAOTA can achieve similar convergence performance when $N_0 = -174\text{dBm/Hz}$. However, when the noise power spectral density is increased to -74dBm/Hz while ensuring that the uplink transmission power of clients remains constant, PAOTA is more robust than COTAF. This is because when optimizing transmission power, PAOTA considers the additive noise parameters of the channel in optimization and thus implements uplink power control adaptively.

Fig. 4 compares the test set accuracy of the three algorithms with respect to communication rounds and training time where we set $N_0 = -174\text{dBm/Hz}$. It can be observed that PAOTA ultimately achieved a prediction accuracy of 83.5%, which is 1.1% higher than that of Local SGD; the prediction accuracy under COTAF is 81%, which is lower than the ideal situation due to the negative impact of the wireless channel on the model accuracy.

From the perspective of training time, the global iteration training time of PAOTA is set to ΔT , while the global iteration training time of Local SGD and COTAF is determined by the client with the longest local computing time in this global round. We list the time and rounds required to achieve

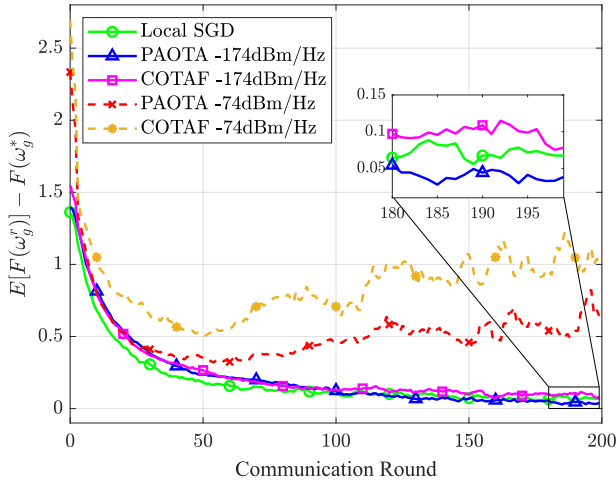


Fig. 3. Train loss in non-IID settings with bandwidth $B=20\text{MHz}$.

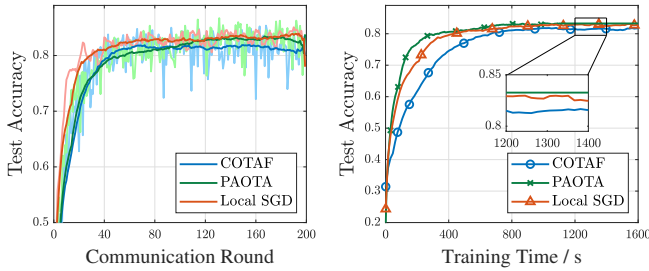


Fig. 4. Test accuracy in non-IID settings.

the target accuracy algorithms in Table I. It can be seen that PAOTA requires more rounds than Local SGD to achieve the target accuracy. However, since the time per round is fixed for PAOTA, while Local SGD needs to wait for all selected clients to complete training before aggregation, PAOTA spends less time to achieve the same target accuracy. For example, PAOTA saves 25% of time to achieve the target accuracy 80% than Local SGD. PAOTA achieves the performance improvement mentioned above because its semi-asynchronous aggregation mechanism can avoid the generation of bottleneck nodes for each global round. Additionally, it controls the weights of expired local models in aggregation to ensure the utilization of data in clients with long local training time.

V. CONCLUSION

In this paper, we first propose a semi-asynchronous mechanism called PAOTA under wireless MAC channels, where the clients suffer from computing heterogeneity. Then, we analyze the convergence behavior of PAOTA and illustrate how the asynchronous strategy and the wireless transmission affect the upper bound of the expected gap between the expected and optimal global loss. Considering the staleness discount introduced by the asynchronous mechanism and the interference effect of local client's update, we model this trade-off problem as the transmission power optimization. In non-IID settings, the simulation results demonstrate that PAOTA can achieve a better performance than other benchmarks in terms

TABLE I
CONVERGENCE TIME

Target Accuracy		50%	60%	70%	80%
PAOTA	round	6	10	18	57
	time/s	36	60	108	342
Local SGD	round	3	6	12	29
	time/s	45.61	78.17	181.24	451.62
COTAF	round	6	12	29	44
	time/s	91.30	181.21	316.75	676.93

of the robustness in terrible wireless condition and convergent speed.

REFERENCES

- [1] B. McMahan, E. Moore, D. Ramage, S. Hampson, and B. A. y Arcas, "Communication-Efficient Learning of Deep Networks from Decentralized Data," in *Proceedings of the 20th International Conference on Artificial Intelligence and Statistics*, PMLR, Apr. 2017, pp. 1273–1282.
- [2] G. Zhu, Y. Wang, and K. Huang, "Broadband Analog Aggregation for Low-Latency Federated Edge Learning," *IEEE Trans. Wireless Commun.*, vol. 19, no. 1, pp. 491–506, Jan. 2020.
- [3] T. Sery and K. Cohen, "On Analog Gradient Descent Learning Over Multiple Access Fading Channels," *IEEE Trans. Signal Process.*, vol. 68, pp. 2897–2911, 2020.
- [4] Y. Shao, D. Gunduz, and S. C. Liew, "Federated Edge Learning With Misaligned Over-the-Air Computation," *IEEE Trans. Wireless Commun.*, vol. 21, no. 6, pp. 3951–3964, Jun. 2022.
- [5] K. Yang, T. Jiang, Y. Shi, and Z. Ding, "Federated Learning via Over-the-Air Computation," *IEEE Trans. Wireless Commun.*, vol. 19, no. 3, pp. 2022–2035, Mar. 2020.
- [6] J.-Y. Gotoh and H. Konno, "Maximization of the Ratio of Two Convex Quadratic Functions over a Polytope," *Computational Optimization and Applications*, vol. 20, no. 1, pp. 43–60, Oct. 2001.
- [7] N. Su and B. Li, "How Asynchronous can Federated Learning Be?," in *2022 IEEE/ACM 30th International Symposium on Quality of Service (IWQoS)*, Jun. 2022, pp. 1–11.
- [8] X. Zhou, Y. Deng, H. Xia, S. Wu, and M. Bennis, "Time-Triggered Federated Learning Over Wireless Networks," *IEEE Trans. Wireless Commun.*, vol. 21, no. 12, pp. 11066–11079, Dec. 2022.
- [9] W. Guo, R. Li, C. Huang, X. Qin, K. Shen, and W. Zhang, "Joint Device Selection and Power Control for Wireless Federated Learning," *IEEE J. Select. Areas Commun.*, vol. 40, no. 8, pp. 2395–2410, Aug. 2022.
- [10] Z. Kou, Y. Ji, X. Zhong, and S. Zhang, "Semi-Asynchronous Federated Edge Learning Mechanism for Over-the-air Computation." 2023, *arXiv:2305.04066*.

APPENDIX A
PROOF OF LEMMA 1

Firstly, we derive the upper bound of the expected square norm of the difference between the local updated model at each SGD iteration and the previous global model $\mathbb{E}[\|\mathbf{w}_g^{r-s_k^r} - \mathbf{w}_{k,\tau-1}^{r-s_k^r}\|_2^2]$ as follow:

$$\begin{aligned}
& \mathbb{E}[\|\mathbf{w}_g^{r-s_k^r} - \mathbf{w}_{k,\tau-1}^{r-s_k^r}\|_2^2] \\
&= \mathbb{E}[\|\eta_t \sum_{l=1}^{\tau-1} \nabla F_k(\mathbf{w}_{k,l-1}^{r-s_k^r}; D_{k,l}^{r-s_k^r})\|_2^2] \\
&\leq \eta_t^2 (\tau-1) \sum_{l=1}^{\tau-1} \mathbb{E}[\|\nabla F_k(\mathbf{w}_{k,l-1}^{r-s_k^r}; D_{k,l}^{r-s_k^r})\|_2^2] \\
&\stackrel{(a)}{=} \eta_t^2 (\tau-1) \sum_{l=1}^{\tau-1} \mathbb{E}[\|\nabla F_k(\mathbf{w}_{k,l-1}^{r-s_k^r}; D_{k,l}^{r-s_k^r}) \\
&\quad - \nabla F_k(\mathbf{w}_{k,l-1}^{r-s_k^r})\|_2^2] \\
&\quad + \eta_t^2 (\tau-1) \sum_{l=1}^{\tau-1} \mathbb{E}[\|\nabla F_k(\mathbf{w}_{k,l-1}^{r-s_k^r})\|_2^2] \\
&\stackrel{(b)}{=} \eta_t^2 (\tau-1)^2 \sigma^2 \\
&\quad + \eta_t^2 (\tau-1) \sum_{l=1}^{\tau-1} \mathbb{E}[\|\nabla F_k(\mathbf{w}_{k,l-1}^{r-s_k^r})\|_2^2] \\
&\leq \eta_t^2 M^2 \sigma^2 + \eta_t^2 M \sum_{l=1}^{\tau-1} \mathbb{E}[\|\nabla F_k(\mathbf{w}_{k,l-1}^{r-s_k^r}) \\
&\quad - \nabla F_k(\mathbf{w}_g^{r-s_k^r}) + \nabla F_k(\mathbf{w}_g^{r-s_k^r})\|_2^2] \\
&\stackrel{(c)}{\leq} \eta_t^2 M^2 \sigma^2 + 2\eta_t^2 M \sum_{l=1}^{\tau-1} \mathbb{E}[\|\nabla F_k(\mathbf{w}_g^{r-s_k^r})\|_2^2] \\
&\quad + 2\eta_t^2 M \sum_{l=1}^{\tau-1} \mathbb{E}[\|\nabla F_k(\mathbf{w}_{k,l-1}^{r-s_k^r}) - \nabla F_k(\mathbf{w}_g^{r-s_k^r})\|_2^2] \\
&\stackrel{(d)}{\leq} \eta_t^2 M^2 \sigma^2 \\
&\quad + 2\eta_t^2 L^2 M \sum_{l=1}^{\tau-1} \mathbb{E}[\|\mathbf{w}_{k,l-1}^{r-s_k^r} - \mathbf{w}_g^{r-s_k^r}\|_2^2] \\
&\quad + 2\eta_t^2 M \sum_{l=1}^{\tau-1} \mathbb{E}[\|\nabla F_k(\mathbf{w}_g^{r-s_k^r}) \\
&\quad - \nabla F_g(\mathbf{w}_g^{r-s_k^r}) + \nabla F_g(\mathbf{w}_g^{r-s_k^r})\|_2^2] \\
&\stackrel{(e)}{\leq} \eta_t^2 M^2 \sigma^2 + 2\eta_t^2 L^2 M \sum_{l=1}^{\tau-1} \mathbb{E}[\|\mathbf{w}_{k,l-1}^{r-s_k^r} - \mathbf{w}_g^{r-s_k^r}\|_2^2] \\
&\quad + 4\eta_t^2 M \sum_{l=1}^{\tau-1} \mathbb{E}[\|\nabla F_k(\mathbf{w}_g^{r-s_k^r}) - \nabla F_g(\mathbf{w}_g^{r-s_k^r})\|_2^2] \\
&\quad + \|\nabla F_g(\mathbf{w}_g^{r-s_k^r})\|_2^2] \\
&\stackrel{(f)}{\leq} \eta_t^2 M^2 \sigma^2 + 4\eta_t^2 M^2 \zeta + 4\eta_t^2 M^2 \beta^2 \mathbb{E}[\|\nabla F_g(\mathbf{w}_g^r)\|_2^2] \\
&\quad + 2\eta_t^2 L^2 M \sum_{l=1}^{\tau-1} \mathbb{E}[\|\mathbf{w}_{k,l-1}^{r-s_k^r} - \mathbf{w}_g^{r-s_k^r}\|_2^2] \quad (40)
\end{aligned}$$

where equality (a) is due to

$$\mathbb{E}[\|\mathbf{x}\|_2^2] = \mathbb{E}[\|\mathbf{x} - \mathbb{E}[\mathbf{x}]\|_2^2] + \|\mathbb{E}[\mathbf{x}]\|_2^2, \quad (41)$$

and

$$\mathbb{E}[\nabla F_k(\mathbf{w}_{k,l-1}^{r-s_k^r}; D_{k,l}^{r-s_k^r})] = \nabla F_k(\mathbf{w}_{k,l-1}^{r-s_k^r}), \quad (42)$$

equality (b) is due to the equation

$$\mathbb{E}[\|\nabla F_k(\mathbf{w}_{k,l-1}^{r-s_k^r}; D_{k,l}^{r-s_k^r}) - \nabla F_k(\mathbf{w}_{k,l-1}^{r-s_k^r})\|_2^2] = \sigma^2, \quad (43)$$

equality (c) and equality (e) are both due to

$$\|\mathbf{x}_1 + \mathbf{x}_2\|_2^2 \leq 2\|\mathbf{x}_1\|_2^2 + 2\|\mathbf{x}_2\|_2^2 \quad (44)$$

equality (d) is by the inequality (11) in Assumption 1, equality (f) is by the inequality (12) in Assumption 2 and the (15) in Assumption 3.

Then, summing both sides of (40) from $\tau = 1$ to M yields

$$\begin{aligned}
& \sum_{\tau=1}^M \mathbb{E}[\|\mathbf{w}_g^{r-s_k^r} - \mathbf{w}_{k,\tau-1}^{r-s_k^r}\|_2^2] \\
&\leq \eta_t^2 M^3 \sigma^2 + 4\eta_t^2 M^3 \zeta + 4\eta_t^2 M^3 \beta^2 \mathbb{E}[\|\nabla F_g(\mathbf{w}_g^r)\|_2^2] \\
&\quad + 2\eta_t^2 L^2 M \sum_{\tau=1}^M \sum_{l=1}^{\tau-1} \mathbb{E}[\|\mathbf{w}_{k,l-1}^{r-s_k^r} - \mathbf{w}_g^{r-s_k^r}\|_2^2] \\
&\leq \eta_t^2 M^3 \sigma^2 + 4\eta_t^2 M^3 \zeta + 4\eta_t^2 M^3 \beta^2 \mathbb{E}[\|\nabla F_g(\mathbf{w}_g^r)\|_2^2] \\
&\quad + 2\eta_t^2 L^2 M^2 \sum_{\tau=1}^M \mathbb{E}[\|\mathbf{w}_{k,\tau-1}^{r-s_k^r} - \mathbf{w}_g^{r-s_k^r}\|_2^2] \quad (45)
\end{aligned}$$

Finally, rearranging the terms in (45) yields Lemma 1.

APPENDIX B
PROOF OF THEOREM 1

According to (9) and the (10) in Assumption 1, we have

$$\begin{aligned}
F(\mathbf{w}_g^{r+1}) &\leq F(\mathbf{w}_g^r) + \langle \mathbf{w}_g^{r+1} - \mathbf{w}_g^r, \nabla F(\mathbf{w}_g^r) \rangle \\
&\quad + \frac{L}{2} \|\mathbf{w}_g^{r+1} - \mathbf{w}_g^r\|_2^2, \quad (46)
\end{aligned}$$

By taking expectation on both sides of (46), we obtain

$$\begin{aligned}
& \mathbb{E}[F(\mathbf{w}_g^{r+1})] \\
&\leq \mathbb{E}[F(\mathbf{w}_g^r)] + \underbrace{\mathbb{E}[\langle \mathbf{w}_g^{r+1} - \mathbf{w}_g^r, \nabla F(\mathbf{w}_g^r) \rangle]}_{A_1} \\
&\quad + \underbrace{\frac{L}{2} \mathbb{E}[\|\mathbf{w}_g^{r+1} - \mathbf{w}_g^r\|_2^2]}_{A_2}. \quad (47)
\end{aligned}$$

Then we bound the terms A_1 and A_2 in the right hand sides of (47) in the following.

A. Bound of A_1

In this section, we derive the bound of A_1 ,

$$\begin{aligned}
A_1 &= \mathbb{E}[\langle \mathbf{w}_g^{r+1} - \mathbf{w}_g^r, \nabla F(\mathbf{w}_g^r) \rangle] \\
&= \mathbb{E}[\langle \tilde{\mathbf{w}}^r - \mathbf{w}_g^r + \sum_{k=1}^K \alpha_k^r \Delta \mathbf{w}_k^r + \tilde{\mathbf{n}}^r, \nabla F(\mathbf{w}_g^r) \rangle] \\
&= \underbrace{\mathbb{E}[\langle \tilde{\mathbf{w}}^r - \mathbf{w}_g^r, \nabla F(\mathbf{w}_g^r) \rangle]}_{B_1} + \underbrace{\mathbb{E}[\langle \tilde{\mathbf{n}}^r, \nabla F(\mathbf{w}_g^r) \rangle]}_{B_3} \\
&\quad + \underbrace{\mathbb{E}[\langle \sum_{k=1}^K \alpha_k^r \Delta \mathbf{w}_k^r, \nabla F(\mathbf{w}_g^r) \rangle]}_{B_2} \quad (48)
\end{aligned}$$

where $b_3 = 0$ because of $\tilde{\mathbf{n}}^r$ is orthogonal to $\nabla F(\mathbf{w}_g^r)$, and $\mathbb{E}[\tilde{\mathbf{n}}^r] = 0$.

We analyze B_1 and B_2 separately. We bound the term B_1 as ,

$$\begin{aligned}
B_1 &= \mathbb{E}[\langle \sum_{k=1}^K \alpha_k^r (\mathbf{w}_g^{r-s_k^r} - \mathbf{w}_g^r), \nabla F(\mathbf{w}_g^r) \rangle] \\
&= \sum_{k=1}^K \alpha_k^r \mathbb{E}[\langle \mathbf{w}_g^{r-s_k^r} - \mathbf{w}_g^r, \nabla F(\mathbf{w}_g^r) \rangle] \\
&\stackrel{(a)}{\leq} \sum_{k=1}^K \alpha_k^r \delta \mathbb{E}[\|\nabla F(\mathbf{w}_g^r)\|_2^2] \\
&= \delta \mathbb{E}[\|\nabla F(\mathbf{w}_g^r)\|_2^2] \quad (49)
\end{aligned}$$

where (a) is due to the (13) in Assumption 3. Then, we study the term B_2 as follow,

$$\begin{aligned}
B_2 &= \mathbb{E}[\langle \sum_{k=1}^K \alpha_k^r \Delta \mathbf{w}_k^r, \nabla F(\mathbf{w}_g^r) \rangle] \\
&= \mathbb{E}[\langle \sum_{k=1}^K \alpha_k^r (-\eta_t \sum_{\tau=1}^M \nabla F_k(\mathbf{w}_{k,\tau-1}^{r-s_k^r}; D_{k,\tau}^{r-s_k^r})), \nabla F(\mathbf{w}_g^r) \rangle] \\
&= -\eta_t \sum_{\tau=1}^M \mathbb{E}[\langle \sum_{k=1}^K \alpha_k^r \nabla F_k(\mathbf{w}_{k,\tau-1}^{r-s_k^r}; D_{k,\tau}^{r-s_k^r}), \nabla F(\mathbf{w}_g^r) \rangle] \\
&\stackrel{(a)}{\leq} -\frac{\eta_t M}{2} \mathbb{E}[\|\nabla F(\mathbf{w}_g^r)\|_2^2] + \eta_t \sum_{k=1}^K \alpha_k^r \sum_{\tau=1}^M \mathbb{E}[\|\nabla F_k(\mathbf{w}_g^{r-s_k^r}) - \nabla F_k(\mathbf{w}_{k,\tau-1}^{r-s_k^r}; D_{k,\tau}^{r-s_k^r})\|_2^2] \\
&\quad + \eta_t \sum_{\tau=1}^M \mathbb{E}[\|\nabla F(\mathbf{w}_g^r) - \sum_{k=1}^K \alpha_k^r \nabla F_k(\mathbf{w}_g^{r-s_k^r})\|_2^2] \\
&\stackrel{(b)}{\leq} -\frac{\eta_t M}{2} \mathbb{E}[\|\nabla F(\mathbf{w}_g^r)\|_2^2] \\
&\quad + \eta_t L^2 \sum_{k=1}^K \alpha_k^r \sum_{\tau=1}^M \mathbb{E}[\|\mathbf{w}_g^{r-s_k^r} - \mathbf{w}_{k,\tau-1}^{r-s_k^r}\|_2^2] \\
&\quad + \underbrace{\eta_t \sum_{\tau=1}^M \mathbb{E}[\|\nabla F(\mathbf{w}_g^r) - \sum_{k=1}^K \alpha_k^r \nabla F_k(\mathbf{w}_g^{r-s_k^r})\|_2^2]}_{C_1}
\end{aligned} \tag{50}$$

where (a) follows the inequality (44) and Jensen's inequality, and (b) follows the (10) in assumption 1 and $\mathbf{w}_g^{r-s_k^r} = \mathbf{w}_k^{r-s_k^r,0}$.

For (49), we further need to bound the term C_1 as follow,

$$\begin{aligned}
C_1 &= \eta_t \sum_{\tau=1}^M \mathbb{E}[\|\nabla F(\mathbf{w}_g^r) - \sum_{k=1}^K \alpha_k^r \nabla F_k(\mathbf{w}_g^{r-s_k^r})\|_2^2] \\
&= \eta_t \sum_{\tau=1}^M \mathbb{E}[\|\sum_{k=1}^K \alpha_k^r (\nabla F(\mathbf{w}_g^r) - \nabla F_k(\mathbf{w}_g^{r-s_k^r}))\|_2^2] \\
&\stackrel{(a)}{\leq} \eta_t \sum_{k=1}^K \alpha_k^r \sum_{\tau=1}^M \mathbb{E}[\|\nabla F(\mathbf{w}_g^r) - \nabla F_k(\mathbf{w}_g^{r-s_k^r})\|_2^2] \\
&= \eta_t \sum_{k=1}^K \alpha_k^r \sum_{\tau=1}^M \mathbb{E}[\|\nabla F(\mathbf{w}_g^r) - \nabla F(\mathbf{w}_g^{r-s_k^r}) \\
&\quad + \nabla F(\mathbf{w}_g^{r-s_k^r}) - \nabla F_k(\mathbf{w}_g^{r-s_k^r})\|_2^2] \\
&\stackrel{(b)}{\leq} \eta_t \sum_{k=1}^K \alpha_k^r \sum_{\tau=1}^M 2\mathbb{E}[\|\nabla F(\mathbf{w}_g^r) - \nabla F(\mathbf{w}_g^{r-s_k^r})\|_2^2] + \\
&\quad \eta_t \sum_{k=1}^K \alpha_k^r \sum_{\tau=1}^M 2\mathbb{E}[\|\nabla F(\mathbf{w}_g^{r-s_k^r}) - \nabla F_k(\mathbf{w}_g^{r-s_k^r})\|_2^2] \\
&\stackrel{(c)}{\leq} 2L\eta_t \sum_{k=1}^K \alpha_k^r \sum_{\tau=1}^M \mathbb{E}[\|\mathbf{w}_g^r - \mathbf{w}_g^{r-s_k^r}\|_2^2] + \\
&\quad 2\eta_t \sum_{k=1}^K \alpha_k^r \sum_{\tau=1}^M \mathbb{E}[\|\nabla F(\mathbf{w}_g^{r-s_k^r}) - \nabla F_k(\mathbf{w}_g^{r-s_k^r})\|_2^2] \\
&\stackrel{(d)}{\leq} 2\eta_t ML^2 \varepsilon^2 + 2\eta_t M \zeta
\end{aligned} \tag{51}$$

where (a) follows the Jensen's Inequality, (b) follows the inequality $\|\mathbf{x}_1 + \mathbf{x}_2\|_2^2 \leq 2\|\mathbf{x}_1\|_2^2 + 2\|\mathbf{x}_2\|_2^2$, (c) follows the (10) in assumption 1, and (d) follows the (12) in Assumption 2 and the (14) in Assumption 3.

Combining (48)-(51), we can obtain

$$\begin{aligned}
A_1 &\leq B_1 + B_2 + B_3 \\
&\leq (\delta - \frac{\eta_t M}{2}) \mathbb{E}[\|\nabla F(\mathbf{w}_g^r)\|_2^2] + 2\eta_t ML^2 \varepsilon^2 + 2\eta_t M \zeta \\
&\quad + \eta_t L^2 \sum_{k=1}^K \alpha_k^r \sum_{\tau=1}^M \mathbb{E}[\|\mathbf{w}_g^{r-s_k^r} - \mathbf{w}_{k,\tau-1}^{r-s_k^r}\|_2^2]
\end{aligned} \tag{52}$$

B. Bound of A_2

In this section, we derive the bound of A_2 ,

$$\begin{aligned}
A_2 &= \mathbb{E}[\|\mathbf{w}_g^{r+1} - \mathbf{w}_g^r\|_2^2] \\
&= \mathbb{E}[\|\tilde{\mathbf{w}}^r - \mathbf{w}_g^r + \sum_{k=1}^K \alpha_k^r \Delta \mathbf{w}_k^r + \tilde{\mathbf{n}}^r\|_2^2] \\
&\stackrel{(a)}{\leq} 2\mathbb{E}[\|\tilde{\mathbf{w}}^r - \mathbf{w}_g^r\|_2^2] + 4\mathbb{E}[\|\sum_{k=1}^K \alpha_k^r \Delta \mathbf{w}_k^r\|_2^2] \\
&\quad + 4\mathbb{E}[\|\tilde{\mathbf{n}}^r\|_2^2] \\
&\stackrel{(b)}{=} \underbrace{2\mathbb{E}[\|\tilde{\mathbf{w}}^r - \mathbf{w}_g^r\|_2^2]}_{B_1} + \underbrace{4\mathbb{E}[\|\sum_{k=1}^K \alpha_k^r \Delta \mathbf{w}_k^r\|_2^2]}_{B_2} \\
&\quad + \frac{4d\sigma_u^2}{(\sum_{k \in K} \alpha_k^r p_k)^2}
\end{aligned} \tag{53}$$

where (a) follows the inequality (44), and (b) follows noise mean square calculation.

We analyze B_1 and B_2 separately. We bound the term B_1 as ,

$$\begin{aligned}
B_1 &= \mathbb{E}[\|\tilde{\mathbf{w}}^r - \mathbf{w}_g^r\|_2^2] \\
&= \mathbb{E}[\|\sum_{k=1}^K \alpha_k^r (\mathbf{w}_g^{r-s_k^r} - \mathbf{w}_g^r)\|_2^2] \\
&= K \sum_{k=1}^K (\alpha_k^r)^2 \mathbb{E}[\|\mathbf{w}_g^{r-s_k^r} - \mathbf{w}_g^r\|_2^2] \\
&\leq \varepsilon^2 K \sum_{k=1}^K (\alpha_k^r)^2
\end{aligned} \tag{54}$$

we study the term B_2 as follow,

$$\begin{aligned}
B_2 &= \mathbb{E}[\|\sum_{k=1}^K \alpha_k^r \Delta \mathbf{w}_k^r\|_2^2] \\
&\stackrel{(a)}{\leq} \sum_{k=1}^K \alpha_k^r \mathbb{E}[\|\Delta \mathbf{w}_k^r\|_2^2] \\
&= \eta_t^2 \sum_{k=1}^K \alpha_k^r \mathbb{E}[\|\sum_{\tau=1}^M \nabla F_k(\mathbf{w}_{k,\tau-1}^{r-s_k^r}; D_{k,\tau}^{r-s_k^r})\|_2^2] \\
&\leq \eta_t^2 M \sum_{k=1}^K \alpha_k^r \sum_{\tau=1}^M \mathbb{E}[\|\nabla F_k(\mathbf{w}_{k,\tau-1}^{r-s_k^r}; D_{k,\tau}^{r-s_k^r})\|_2^2] \\
&\stackrel{(b)}{=} \eta_t^2 M \sum_{k=1}^K \alpha_k^r \sum_{\tau=1}^M \mathbb{E}[\|\nabla F_k(\mathbf{w}_{k,\tau-1}^{r-s_k^r}; D_{k,\tau}^{r-s_k^r}) \\
&\quad - \nabla F_k(\mathbf{w}_{k,\tau-1}^{r-s_k^r})\|_2^2] \\
&\quad + \eta_t^2 M \sum_{k=1}^K \alpha_k^r \sum_{\tau=1}^M \mathbb{E}[\|\nabla F_k(\mathbf{w}_{k,\tau-1}^{r-s_k^r})\|_2^2] \\
&\stackrel{(c)}{\leq} \eta_t^2 M^2 \sigma^2 \\
&\quad + \eta_t^2 M \sum_{k=1}^K \alpha_k^r \sum_{\tau=1}^M \mathbb{E}[\|\nabla F_k(\mathbf{w}_{k,\tau-1}^{r-s_k^r})\|_2^2] \\
&\stackrel{(d)}{=} \eta_t^2 M^2 \sigma^2 + \eta_t^2 M \sum_{k=1}^K \alpha_k^r \sum_{\tau=1}^M \mathbb{E}[\|\nabla F_k(\mathbf{w}_{k,\tau-1}^{r-s_k^r}) \\
&\quad - \nabla F_k(\mathbf{w}_g^{r-s_k^r}) + \nabla F_k(\mathbf{w}_g^{r-s_k^r})\|_2^2] \\
&\stackrel{(e)}{\leq} \eta_t^2 M^2 \sigma^2 + 2\eta_t^2 M^2 \sum_{k=1}^K \alpha_k^r \mathbb{E}[\|\nabla F_k(\mathbf{w}_g^{r-s_k^r})\|_2^2]
\end{aligned}$$

$$\begin{aligned}
& + 2M\eta_t^2 \sum_{k=1}^K \alpha_k^r \sum_{\tau=1}^M \mathbb{E}[\|\nabla F_k(\mathbf{w}_{k,\tau-1}^{r-s_k^r}) \\
& - \nabla F_k(\mathbf{w}_g^{r-s_k^r})\|_2^2] \\
& \stackrel{(f)}{\leq} \eta_t^2 M^2 \sigma^2 \\
& + 2M\eta_t^2 L^2 \sum_{k=1}^K \alpha_k^r \sum_{\tau=1}^M \mathbb{E}[\|\mathbf{w}_{k,\tau-1}^{r-s_k^r} - \mathbf{w}_g^{r-s_k^r}\|_2^2] \\
& + 2\eta_t^2 M^2 \sum_{k=1}^K \alpha_k^r \mathbb{E}[\|\nabla F_k(\mathbf{w}_g^{r-s_k^r}) - \nabla F(\mathbf{w}_g^{r-s_k^r}) \\
& + \nabla F(\mathbf{w}_g^{r-s_k^r})\|_2^2] \\
& \stackrel{(g)}{\leq} \eta_t^2 M^2 \sigma^2 + 4\eta_t^2 M^2 \zeta + 4\eta_t^2 M^2 \beta^2 \mathbb{E}[\|\nabla F(\mathbf{w}_g^r)\|_2^2] \\
& + 2M\eta_t^2 L^2 \sum_{k=1}^K \alpha_k^r \sum_{\tau=1}^M \mathbb{E}[\|\mathbf{w}_{k,\tau-1}^{r-s_k^r} - \mathbf{w}_g^{r-s_k^r}\|_2^2]
\end{aligned} \tag{55}$$

where (a) follows Jensen's Inequality, (b) and (d) follow equality (41), (c) follows the equality (43), (e) follow equality (44), (f) follows the (11) in Assumption 1, and (g) follows the (12) in Assumption 2 and (15) in Assumption 3.

Combining (53)-(55), we can obtain

$$\begin{aligned}
A_2 & \leq 2B_1 + 4B_2 + \frac{4d\sigma_u^2}{(\sum_{k \in K} a_k^r p_k^r)^2} \\
& \leq \frac{4d\sigma_u^2}{(\sum_{k \in K} a_k^r p_k^r)^2} + 4\eta_t^2 M^2 \sigma^2 + 16\eta_t^2 M^2 \zeta \\
& + 16\eta_t^2 M^2 \beta^2 \mathbb{E}[\|\nabla F(\mathbf{w}_g^r)\|_2^2] + 2\varepsilon^2 K \sum_{k=1}^K (\alpha_k^r)^2 \\
& + 8M\eta_t^2 L^2 \sum_{k=1}^K \alpha_k^r \sum_{\tau=1}^M \mathbb{E}[\|\mathbf{w}_{k,\tau-1}^{r-s_k^r} \\
& - \mathbf{w}_g^{r-s_k^r}\|_2^2]
\end{aligned} \tag{56}$$

C. Proof of Theorem 1

Combining (47), (52) and (56), we obtain

$$\begin{aligned}
& \mathbb{E}[F(\mathbf{w}_g^{r+1})] \\
& \leq \mathbb{E}[F(\mathbf{w}_g^r)] + A_1 + \frac{L}{2} A_2 \\
& \stackrel{(a)}{\leq} \mathbb{E}[F(\mathbf{w}_g^r)] + (\delta - \frac{\eta_t M}{2} + 8L\eta_t^2 M^2 \beta^2 \\
& + (\eta_t L^2 + 4M\eta_t^2 L^3) \frac{4\eta_t^2 M^3 \beta^2}{1 - 2\eta_t^2 M^2}) \mathbb{E}[\|\nabla F(\mathbf{w}_g^r)\|_2^2] \\
& + 2\eta_t M L^2 \varepsilon^2 + 2\eta_t M \zeta + L\varepsilon^2 K \sum_{k=1}^K (\alpha_k^r)^2 \\
& + 2L\eta_t^2 M^2 \sigma^2 + 8L\eta_t^2 M^2 \zeta \\
& + (\eta_t L^2 + 4M\eta_t^2 L^3) \frac{\eta_t^2 M^3 \sigma^2 + 4\eta_t^2 M^3 L^2 \zeta}{1 - 2\eta_t^2 M^2 L^2} \\
& + \frac{2Ld\sigma_u^2}{(\sum_{k \in K} a_k^r p_k^r)^2}
\end{aligned} \tag{57}$$

where (a) follows (18) in Lemma 1.

By subtracting F^* at both sides of (57), we have

$$\mathbb{E}[F(\mathbf{w}_g^{r+1}) - F^*] \stackrel{(a)}{\leq} A^r \mathbb{E}[F(\mathbf{w}_g^r) - F^*] + G^r \tag{58}$$

with

$$\begin{aligned}
A^r & = 1 + 2L\delta - L\eta M + 8L^2 \eta^2 M \beta^2 \\
& + (\eta L^2 + 4M\eta^2 L^3) \frac{8L\eta^2 M^3 \beta^2}{1 - 2\eta^2 M^2 L^2},
\end{aligned} \tag{59}$$

and

$$\begin{aligned}
G^r & = \underbrace{(2\eta M + 8L\eta M^2 + \frac{4\eta^2 M^3 L^2 (\eta L^2 + 4M\eta^2 L^3)}{1 - 2\eta^2 M^2 L^2})}_{(a)} \zeta \\
& + \underbrace{2\eta M L^2 \varepsilon^2 + (2\eta^2 L M^2 + \frac{(\eta L^2 + 4M\eta^2 L^3) \eta^2 M^3}{1 - 2\eta^2 M^2 L^2})}_{(b)} \sigma^2 \\
& + \underbrace{L\varepsilon^2 K \sum_{k=1}^K (\alpha_k^r)^2}_{(d)} + \underbrace{\frac{2Ld\sigma_n^2}{(\sum_{k=1}^K b_k^r p_k^r)^2}}_{(e)},
\end{aligned} \tag{60}$$

where (a) follows (19) in Lemma 2.

Assume the FL algorithm terminates after R rounds, given an initial global model \mathbf{w}_1 , we carry out recursions as

$$\begin{aligned}
& \mathbb{E}[F(\mathbf{w}_g^{R+1}) - F^*] \\
& \leq A^R \mathbb{E}[F(\mathbf{w}_g^R) - F^*] + G^R \\
& \leq A^R A^{R-1} \mathbb{E}[F(\mathbf{w}_g^{R-1}) - F^*] + G^{R-1} + G^R \\
& \leq \dots \\
& \leq \prod_{t=1}^R A^t \mathbb{E}[F(\mathbf{w}_g^1) - F^*] + \sum_{t=1}^R (\prod_{i=r+1}^R A^i) G^r + G^R
\end{aligned} \tag{61}$$

Thus, this completes the proof.